ISSN (Print) 1226-1750
ISSN (Online) 2233-6656
Journal of Magnetics 20(4), 336-341 (2015) http://dx.doi.org/10.4283/JMAG.2015.20.4.336

Preparation and Magnetic Properties of MnBi Alloy and its Hybridization with NdFeB

Nguyen Xuan Truong and Nguyen Van Vuong*

Institute of Materials Science, Vietnam Academy of Science and Technology, Hanoi 10000, Vietnam

(Received 7 August 2015, Received in final form 10 October 2015, Accepted 13 October 2015)

MnBi alloys were fabricated by arc melting and annealing at 573 K. The heat treatment enhanced the content of the low-temperature phase (LTP) of MnBi up to 83 wt%. The Bi-excess assisted LTP MnBi alloys were used in the hybridization with the Nd-Fe-B commercial Magnequench ribbons to form the hybrid magnets (100-*x*)NdFeB/*x*MnBi, *x* = 20, 30, 40, 50, and 80 wt%. The as-milled powder mixtures of Nd-Fe-B and MnBi were aligned in a magnetic field of 18 kOe and warm-compacted to anisotropic and dense bulk magnets at 573 K by 2,000 psi for 10 min. The magnetic ordering of two hard phase components strengthened by the exchange coupling enhanced the Curie temperature (T_c) of the magnet in comparison to that of the powder mixture sample. The prepared hybrid magnets were highly anisotropic with the ratio $M_r/M_s > 0.8$. The exchange coupling was high, and the coercivity ${}_iH_c$ of the magnets was ~11-13 kOe. The maximum value of the energy product $(BH)_{max}$ was 8.4 MGOe for the magnet with *x* = 30%. The preparation of MnBi alloys and hybrid magnets are discussed in details.

Keywords : MnBi alloy, NdFeB/MnBi hybrid magnets, exchange coupling, magnetic properties.

1. Introduction

The price of rare-earth elements has increased sharply (e.g., for NdPr alloys, the price was increased by 565% in 2011 in comparison to that in 2010 [1]); therefore, the development of rare-earth-free permanent magnets is becoming more important, and MnBi-based magnets have received renewed research interest [2-5].

Attempts for preparing high-performance single-phase MnBi alloys and bulk magnets have been intensively carried out during the last years [3, 6-15]. The phase responsible for the ferromagnetism of MnBi is formed only at temperature < 613 K [12] and is called as the low-temperature phase (LTP). The complexity of the phase diagram of Mn-Bi system leads to the multiphase segregation of MnBi, Bi, and Mn in MnBi alloys. This segregation prevents to prepare single LTP MnBi alloys, and the MnBi annealed alloys are always Bi-excess assisted LTP MnBi.

From the other point of view, the Bi-excess assisted LTP MnBi alloys can function as a metallic binder to hybridize LTP MnBi with rare earth containing hard phases to form dense hybrid magnets. Despite the medium spontaneous magnetization J_s (~8.2 kG) of MnBi, it has a high magneto-crystalline anisotropy energy of 0.9 MJ/m^3 [2], and especially the positive temperature coefficient of coercivity (${}_iH_c$) attributes hybridization to be promising for high temperature and low-cost hybrid permanent magnet applications. The research on this type of magnets is currently under development [16-18].

In this study, we present the results of our study on Nd-Fe-B/MnBi hybrid magnets. Different from the study reported by Cao S. *et al.* [16], high magnetization and low coercivity MnBi powders were selected for the first component of hybrid magnets. The ground Nd-Fe-B commercial Magnequench (MQ) ribbons (MQP-14-12) serves as the second component of magnets. These powders were well hybridized into dense magnets during the low-temperature and short-time sintering process occurred in the Bi-excess melting medium. The exchange coupling existing between these two magnetically hard phases smoothes hysteresis loops, keeps the coercivity of magnets high. The current maximum value of the energy product $(BH)_{max}$ of the prepared hybrid magnets reached 8.4 MGOe. The preparations of MnBi alloys and hybrid magnets are discussed in details.

*Corresponding author: Tel: +84-965088111
Fax: +84-04-38360705, e-mail: vuongnv@ims.vast.ac.vn

2. Materials and Methods

The starting materials consisted of ground Nd-Fe-B MQ ribbons and home-made MnBi powders. To prepare MnBi alloys, high-purity (99.99%) Mn and Bi in the atomic ratio Mn:Bi of 1:1 were molten by the arc melting. The ingot was molten thrice to achieve relatively homogeneous samples. The arc-melted alloys were annealed at 573 K for different times under argon by using the profiled heat treatment method [11], in which the samples are subjected to a temperature of 573 K superposed by a small temperature gradient (gradT) of ~2 K/cm along the height of samples.

To prepare Nd-Fe-B/MnBi hybrid magnets of (100-*x*)Nd-Fe-B/*x*MnBi with *x* being a weight percentage, the Nd-Fe-B MQ ribbons and MnBi annealed alloys were first ground separately and mixed in the selected ratio, ball-milled, and sieved. The as-sieved powders were in-mold aligned in 18 kOe magnetic field and warm-compacted at 573 K by 2,000 psi uniaxial pressure for 10 min. The pressing direction was perpendicular to the magnetic alignment direction.

The prepared hybrid magnets were dense with the mass density varied from 5.6 to 8.5 g/cm^3 depending on the chosen *x* values. The phase composition and texture of the magnets were examined by XRD measured using an X-ray diffractometer (Siemens D5000). The microstructures and EDX results of the magnets were investigated by using an electron microscopy system Jeol 6490–JED 2300. The DSC traces (measured by the TGA-DSC Labsys Evo system) were used to examine the T_c of magnet and powder samples proving the existence of an exchange coupling between the two hard magnetic phases. The magnetic properties of the obtained magnets were measured by the pulsed field magnetometer (PFM). For the loop measurements, samples were cut from magnets into the cubic shaped pieces. The loops were measured along both the parallel and perpendicular to the alignment direction. The measured results were corrected by the demagnetization factor for cubic shape.

3. Results and Discussion

3.1. MnBi and Nd-Fe-B components used for making hybrid magnets

According to the phase diagram of $Mn_yBi_{(100-y)}$ system [12], MnBi phase was formed via a low temperature peritectic reaction process during the solidification process. The arc-melted and annealed (in the temperature range 544-613 K) alloys always consist of the following different phases: ferromagnetic LTP MnBi, Bi and Mn for $y > 23$ or LTP MnBi and Bi phases for $y \leq 23$.

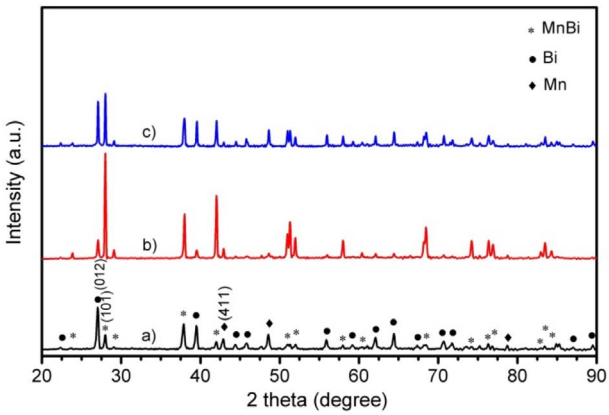

Fig. 1. (Color online) XRD patterns of the powders ground from (a) the MnBi arc-melted alloy, (b) the MnBi alloy annealed at 573 K with gradT ~2 K/cm and c) the MnBi alloy annealed at 573 K with gradT = 0 K/cm. Three strongest peakes (012) of Bi, (101) of LTP MnBi and (411) of Mn are marked.

The XRD patterns of the powders ground from MnBi arc-melted and annealed alloys are shown in Fig. 1, where the three strongest peaks Bi(012), MnBi(101), and Mn(411) are marked. The arc-melted MnBi alloy was solidified into three phases, LTP MnBi, Bi, and Mn, with Bi as the dominated phase (Fig. 1a with the highest peak Bi(012)). In contrast, for the annealed alloy, the content of MnBi LTP significantly increased (Fig. 1b). The annealing process significantly enhanced the MnBi LTP content, and the ratio α of the intensities of the two strongest peaks of MnBi and Bi, $\alpha = I_{MnBi(101)}/I_{Bi(012)}$, increased from 0.32 for the arc-melted alloy to 5.8 for the annealed one.

The content γ of the MnBi LTP of the annealed samples

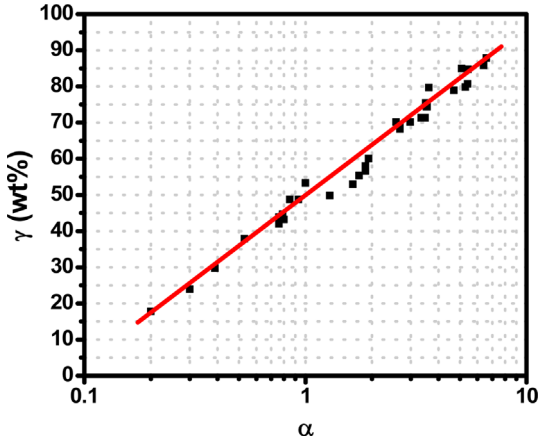

Fig. 2. (Color online) The calibration curve between the ratio α of the two strongest peaks of MnBi (101) and Bi (012) of the XRD patterns and the LTP contents γ.

was instantly estimated by using the mentioned ratio α and the calibration curve describing the relationship between α and MnBi LTP content γ presented in Fig. 2.

To build this calibration curve, 34 samples of MnBi alloys, which were arc melted and annealed for different times, were chosen. The LTP contents γ of these samples were determined by using the Rietveld refinements performed with three input phases of MnBi (PDF#03-065-8164), Bi (PDF#01-071-4643), and Mn (PDF#01-089-2412). The error of LTP content estimation is ~5%. The dependence between γ and logarithmically scaled ratio α has been squared in Fig. 2. The linear behavior of this dependence proves the diffusion mechanism of MnBi LTP phase formation from the Bi and Mn phases. The fitting curve serves as a calibration curve and can be expressed by the following equation:

$$\gamma = 44.6 + 51.3 \log \alpha$$

The MnBi alloy used for making hybrid magnets was annealed for 20 h. Its ratio α was 5.8, corresponding to 83 wt% LTP content γ. This γ value consists with the value of 82 wt% when one compares the magnetization value of 6.7 kG of the MnBi hand-ground powder sample measured at 40 kOe (Fig. 3) and the spontaneous magnetization of 8.2 kG of LTP MnBi [2]. Notably, the above mentioned superposed temperature gradient improved the formation of MnBi LTP. In the case of gradT = 0 K/cm, the ratio α is 1.21 (Fig. 1c), corresponding to the value of only 49 wt% LTP content, which is < 83 wt% obtained for the sample annealed at a gradT of 2 K/cm. This improvement is attributed to the temperature gradient driven diffusion process between Bi and Mn to form the LTP MnBi. The similar process has been studied theoretically and experimentally [19-21].

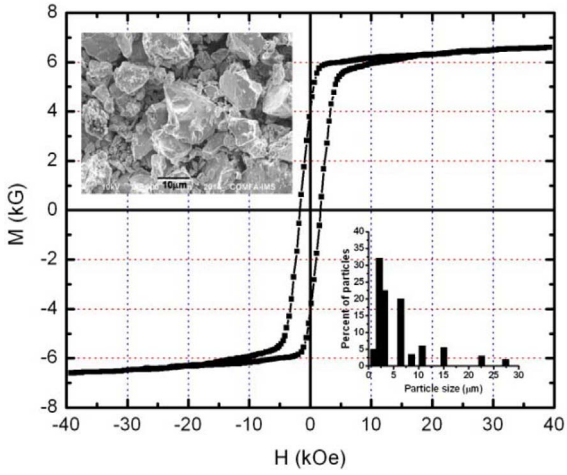

Fig. 3. (Color online) The magnetization loop of MnBi powder of the hand-ground MnBi annealed alloy. Its SEM image and particle size distribution are shown in the insets. The average particle size is in the range 2-6 μm.

The SEM image and particle distribution of the hand-ground MnBi powder are shown in the insets of Fig. 3. The MnBi particles in the size range 2-6 μm were selected to fit the average size of 10 μm of the hand-ground Nd-Fe-B MQ ribbons for the next ball-milling process. The coercivity of these MnBi micrometer-size powders is 2 kOe. The loop of the ground MQ ribbons was also measured by the PFM, indicating M_s = 11.4 kG, ${}_iH_c$ = 13.8 kOe, and $(BH)_{max}$ = 9.5 MGOe.

3.2. Exchange coupling in hybrid magnets

The hybridization between the two hard magnetic materials Nd-Fe-B and MnBi of the ball-milled and sieved Nd-Fe-B/MnBi mixture was made by the 18 kOe-magnetic-field alignment and 573 K-warm-compaction.

According to the study by Muller M. W. and Indeck R. S. [22], inside a system of magnetic grains, the exchange energy affecting *i*-th grain from a group of the nearest neighbor grains *j* is proportional to the angle between the magnetizations $\boldsymbol{m}_i$ and $\boldsymbol{m}_j$, the magnetocrystalline constant K_a and exchange energy constant A of grains *j*, and the fraction f of the facing surfaces in contacts between the grain *i* and neighboring grains *j*.

In the investigated case, the alignment between $\boldsymbol{m}_i$ and $\boldsymbol{m}_j$ of NdFeB and MnBi grains was supported by the field alignment process. The fraction f was improved by the warm compaction under a pressure of 2,000 psi. The K_a and A constants are significant for both the NdFeB and MnBi materials.

Notably, in the case of hard/soft composite magnets, the exchange coupling is critically required for hardening the soft phase grains, and the soft phase grains should be hardened in this manner only if their size is of the domain wall length of the hard phase. However, in contrast, in the case of hard/hard hybrid magnets, the exchange coupling interaction between the two hard phases is required only to keep a good interface magnetic interaction to support the magnetic ordering of the two hard phases to form a unique magnet. Because of the significant constants A of both the hard phases, the exchange coupling in hard/hard hybrid magnets is mutual, and therefore the grain size requirement for hard/hard hybrid magnets decreases at least twice in comparison to that of hard/soft composite magnets.

The differential scanning calorimetry (DSC) measurements manifest the phase transitions including the magnetic ones; therefore, the T_c can be determined by DSC measurements [23]. For ferromagnetic materials, T_c manifests the magnetic ordering and relates to the transition

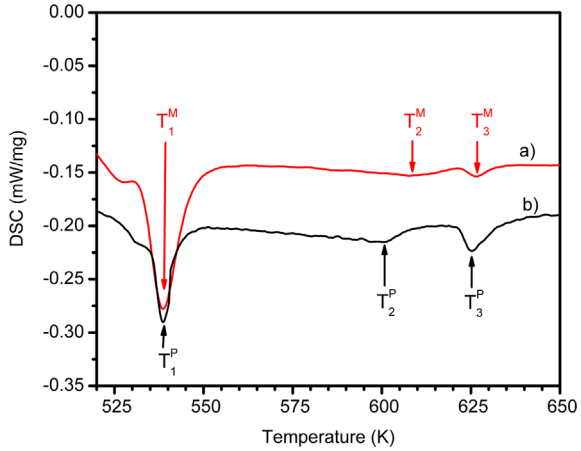

Fig. 4. (Color online) DSC traces of 70%NdFeB/30%MnBi magnet (a) and powder (b) samples.

from the ferromagnetic phase to the paramagnetic one or vice versa. Once an exchange coupling exists in the hybrid magnets, this coupling should strengthen the magnetic ordering of the two hard phases, and thus in turn should increase the T_c of these two hard phases of hybrid magnets in comparison to those of the powder mixture samples with the same composition value x.

This tendency was clearly observed in the DSC traces of 70%Nd-Fe-B/30%MnBi powder and magnet samples presented in Fig. 4. To check any possible effect of the composition changes of magnet and powder samples in the DSC trace shifts, XRD patterns of these two samples were carefully measured (Fig. 5). However, no change in the phases of these two samples was observed in their XRD patterns, and the shifts of the peaks of the DSC traces were clearly recognized.

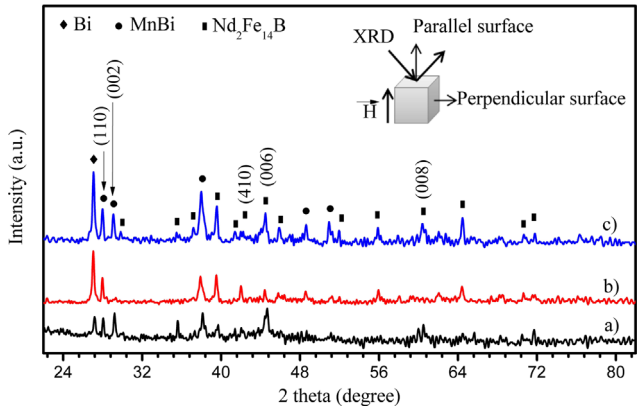

Fig. 5. (Color online) The room-temperature XRD patterns of: the sample of 70%NdFeB/30%MnBi powders embedded in the epoxy resin and aligned under 18 kOe magnetic field and measured on the surface parallel to the alignment direction (a), the bulk 70%NdFeB/30%MnBi hybrid magnet and measured on its surfaces perpendicular (b) and parallel (c) to the alignment direction.

The DSC traces consist of three typical endothermic peaks $T_{1,2,3}$ with the upper indexes M for magnet and P for powder samples. It is easily understood that the first peak corresponds to the melt of Bi, and the 2nd and 3rd peaks correspond to the T_c of NdFeB and MnBi, respectively. The first peak is conserved for the both the powder and magnet samples, whereas the second and third peaks of the magnet sample shifted to the higher temperatures in comparison to that of the powder sample. These T_c-shifts are the conclusive proof of the existence of the exchange coupling between NdFeB and MnBi grains. Because the magnetic ordering in MnBi is more stable than that in NdFeB, the exchange coupling should result in larger T_c-shift for NdFeB than that of MnBi. This effect is clearly observed in Fig. 4 where the peak T_2 is shifted from 601 to 609 K, but the peak T_3 is shifted only from 625 K to 627 K.

3.3. Properties of hybrid magnets

By the exchange coupling, the high coercivity of NdFeB improves the coercivity of hybrid magnets despite the low coercivity of MnBi. The coupling also helps in smoothing the hysteresis loop of the magnets. In principle, the magnetization M_s of hybrid magnets should be lower than that of NdFeB, but the remanent M_r of hybrid magnets can be waited on the accepted level supported by the activated exchange coupling.

The microstructure of the prepared hybrid magnets was investigated by SEM. Fig. 6 shows the SEM image of the dense compact of the fresh breaking surface of the magnet.

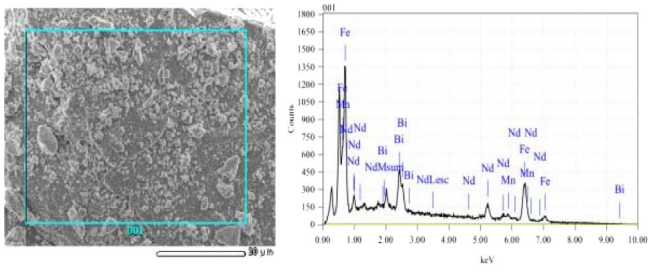

ZAF Method Standardless Quantitative Analysis
Fitting Coefficient : 0.5717

Element	(keV)	Mass%	Error%	Atom%
Mn K	5.894	4.04	2.18	5.46
Fe K	6.398	57.90	2.86	77.05
Nd L	5.227	24.74	3.81	12.75
Bi M	2.419	13.33	1.15	4.74
Total		100.00		100.00

Fig. 6. (Color online) SEM image of the fresh breaking surface of 70%NdFeB/30%MnBi hybrid magnet. The EDX result taken in the wide area marked by the frame reveals that the magnet consists of Nd-rich NdFeB and Mn-rich MnBi particles.

This close packing was formed because of the melted Bi-excess included in the MnBi powder. The magnet mass density (ρ) increased from 5.6 to 8.5 g/cm^3 by increasing the value of x from 0 to 100%. These ρ values are larger than the typical density 5.6 g/cm^3 of commercial bonded NdFeB magnets with an inorganic binder.

Except for boron, the averaged elemental contents of Nd, Fe, Mn, and Bi were determined by the EDX analysis performed on a wide area of sample. The obtained result proved that the Nd-rich $Nd_2Fe_{14}B$ and Mn-rich MnBi compositions were formed during the magnet warm compactions. The Nd-rich $Nd_2Fe_{14}B$ phase is typical for MQ ribbons. The Mn-rich MnBi phase is the consequence of the 573 K warm compaction of magnets. The Bi-excess of the MnBi powder became a binder to form dense hybrid magnets. Because of the low melting temperature of 544 K, under a pressure of 2,000 psi and heat-treatment at 573 K, some fraction of the melted Bi immigrated to the outer surfaces leaving the Mn-rich MnBi phase inside magnets.

Good alignment ability is one of the advantages of LTP MnBi, attributed to its hexagonal structure. This ability improves the alignment of hybrid magnets. The alignment effect was investigated by the XRD patterns measured on the magnet surfaces perpendicular and parallel to the direction of the magnetic field used during the magnets compaction. These patterns are presented in Fig. 5. To assess the alignment effect quantitatively, the ratio between the peak intensities (002) and (101) of MnBi LTP, $\zeta = I_{(002)}/I_{(101)}$, was taken into account for estimating the texture of the crystallites aligned along the easy axis (00l). For the fully isotropic MnBi powder sample, ζ equals 0.102. In the case of the magnet with x = 30%, for the parallel surface (curve c, Fig. 5) ζ = 0.9, which is five times larger than the value 0.18 for the perpendicular surface (curve b, Fig. 5). Notably, in the in-epoxy aligned powder sample (curve a, Fig. 5), where the MnBi particles can freely rotate under action of the alignment magnetic field of 18 kOe, the ratio ζ is large and equals 1.4.

In Fig. 5, together with the texture of the MnBi phase, the texture of the $Nd_2Fe_{14}B$ phase shows the enhanced (006) and (008) peaks. These textures of these two phases allow the hybrid magnets being anisotropic, thus improving the ratio M_r/M_s of the magnet hysteresis loops.

The typical magnetization hysteresis loop of the prepared hybrid magnets is presented in Fig. 7. For this magnet, the x, ρ, magnetization M_s at 40 kOe, and ratio M_r/M_s were 30%, 6.5 g/cm^3, 7.6 kG, and 0.81, respectively. The loop of the magnets was smooth because of the exchange coupling existing between the Nd-Fe-B and MnBi grains. The magnet was highly anisotropic leading

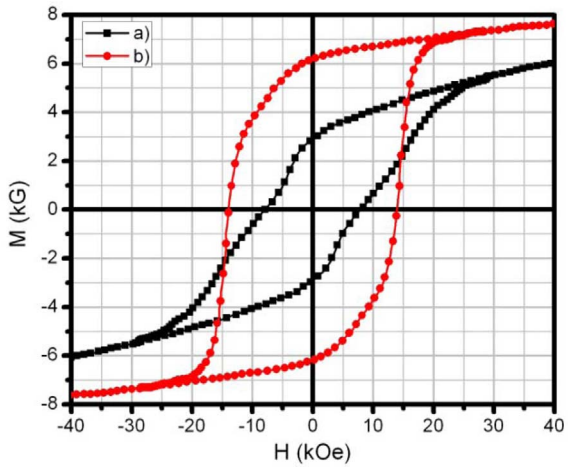

Fig. 7. (Color online) The magnetization loops of 70%NdFeB/30%MnBi hybrid magnet measured in the directions perpendicular (a) and parallel (b) to the alignment direction.

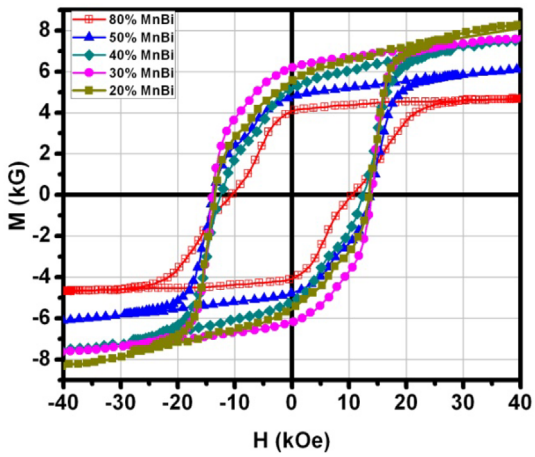

Fig. 8. (Color online) The magnetization loops *M(H)* of the prepared hybrid magnets. The magnetized field H was parallel to the alignment direction of magnets.

to a significant difference between the loops measured with the magnetized field parallel and perpendicular to the alignment direction.

The magnetization loops of the hybrid magnets with x = 20, 30, 40, 50, and 80 wt% are plotted in Fig. 8. Obviously, the M_s of the magnets decreased with increasing fraction x of MnBi. However, despite the above mentioned low $_iH_c$ value of 2 kOe of MnBi, the exchange coupling helps keeping the $_iH_c$ of magnets >10 kOe. The ratio M_r/M_s was kept > 0.8 for all the prepared hybrid magnets. The MnBi fraction affects the shape of the 2nd quadrant loop curves and leads to the maximum value of $_bH_c$ for x = 30%, and thus to the maximum value of $(BH)_{max}$= 8.4 MGOe for 70%NdFeB/30%MnBi hybrid magnet.

4. Conclusions

The hybrid magnets (100-*x*)NdFeB/*x*MnBi were prepared by the 18 kOe-field alignment of a mixture of Nd-Fe-B MQ ribbons and MnBi powder and warm-compaction under 2,000 psi and 573 K for 10 min. This technique allows preparing dense magnets with the mass density in the range 5.6-8.5 g/cm^3 depending on the *x* values. The shifts to the higher T_c temperatures of Nd-Fe-B and MnBi hard phases observed in the DSC traces for the magnet sample in comparison to that of the powder sample proved the existence of the exchange coupling between these two phases in the prepared hybrid magnets. This coupling made the hysteresis loops of magnets smooth, keeping the ${}_iH_c$ of the magnets >10 kOe, despite the low coercivity value of 2 kOe of MnBi. The good alignment of MnBi particles improved the texture of the hybrid magnets; therefore, the prepared hybrid magnets are highly anisotropic with the ratio M_r/M_s >0.8. The magnet 70%NdFeB/30%MnBi has the highest $(BH)_{max}$ = 8.4 MGOe. The performance of Nd-Fe-B/MnBi hybrid magnets can be improved further by increasing the ratio M_r/M_s and enhancing the balance between M_r and ${}_bH_c$ of magnets. The obtained results prove that the proposed type of hybrid magnets is promising and should be considered as a good candidate for high-temperature applications of permanent magnets.

Acknowledgements

This research is funded by the Key National Laboratory of the Institute of Materials Science, code: CSTĐ02.14 and by the Vietnam National Foundation for Science and Technology Development (NAFOSTED) under grant number 103.02-2014.28.

References

[1] Ding Kaihong, EPJ Web of Conferences **75**, 04005 (2014).
[2] J. M. D. Coey, Scripta Materialia **67**, 524 (2012).
[3] P. Kharel, V. R. Shah, R. Skomski, J. E. Shield, and D. J. Sellmyer, IEEE Trans. Magn. **49**, 3318 (2013).
[4] M. J. Kramer, R. W. McCallum, I. A. Anderson, and S. Constantinides, JOM **64**, 752 (2012).
[5] V. Ly, X. Wu, L. Smillie, T. Shoji, A. Kato, A. Manabe, and K. Suzuki, J. Alloys Compd. **615**, Supplement 1, S285 (2014).
[6] C. Chinnasamy, M. M. Jasinski, A. Ulmer, Li Wanfeng, G. Hadjipanayis, and Liu, Jinfang, IEEE Trans. Magn. **48**, 3641 (2012).
[7] J. Cui, J. P. Choi, G. Li, E. Polikarpov, J. Darsell, M. J. Kramer, N. A. Zarkevich, L. L. Wang, D. D. Johnson, M. Marinescu, Q. Z. Huang, H. Wu, N. V. Vuong, and J. P. Liu, J. Appl. Phys. **115**, 17A743 (2014).
[8] J. Cui, J. P. Choi, G. Li, E. Polikarpov, J. Darsell, N. Overman, M. Olszta, D. Schreiber, M. Bowden, T. Droubay, M. J. Kramer, N. A. Zarkevich, L. L. Wang, D. D. Johnson, M. Marinescu, I. Takeuchi, Q. Z. Huang, H. Wu, H. Reeve, N. V. Vuong, and J. P. Liu, J. Physics: Condensed Matter **26**, 064212 (2014).
[9] V. Vuong Nguyen, N. Poudyal, X. B. Liu, J. Ping Liu, K. Sun, M. J. Kramer, and J. Cui, Materials Research Express **1**, 036108 (2014).
[10] N. V. Rama Rao, A. M. Gabay, and G. C. Hadjipanayis, J. Phys. D: Appl. Phys. **46**, 062001 (2013).
[11] Van Vuong, Nguyen, Poudyal, N., Xubo, Liu, Liu, J. P., Kewei, Sun, Kramer, M. J., and Jun, Cui, IEEE Trans. Magn. **50**, 1 (2014).
[12] Y. Mitsui, K. Koyama, and K. Watanabe, Mater. Trans. **54**, 242 (2013).
[13] Y. B. Yang, X. G. Chen, S. Guo, A. R. Yan, Q. Z. Huang, M. M. Wu, D. F. Chen, Y. C. Yang, and J. B. Yang, J. Magn. Magn. Mater. **330**, 106 (2013).
[14] Y. B. Yang, X. G. Chen, R. Wu, J. Z. Wei, X. B. Ma, J. Z. Han, H. L. Du, S. Q. Liu, C. S. Wang, Y. C. Yang, Y. Zhang, and J. B. Yang, J. Appl. Phys. **111**, 07E312 (2012).
[15] D. T. Zhang, W. T. Geng, M. Yue, W. Q. Liu, J. X. Zhang, J. A. Sundararajan, and Y. Qiang, J. Magn. Magn. Mater. **324**, 1887 (2012).
[16] S. Cao, M. Yue, Y. X. Yang, D. T. Zhang, W. Q. Liu, J. X. Zhang, Z. H. Guo, and W. Li, J. Appl. Phys. **109**, 07A740 (2011).
[17] N. V. R. Rao, A. M. Gabay, and G. C. Hadjipanayis, IEEE Trans. Magn. **49**, 3255 (2013).
[18] Y. B. Yang, J. Z. Wei, X. L. Peng, Y. H. Xia, X. G. Chen, R. Wu, H. L. Du, J. Z. Han, C. S. Wang, Y. C. Yang, and J. B. Yang, J. Appl. Phys. **115**, 17A721 (2014).
[19] Ryuichi Habu, Mater. Trans. JIM **40**, 1355 (1999).
[20] A. Feygenson and J. N. Zemel, Thin Solid Film **157**, 49 (1988).
[21] R. R. Mohanty, J. E. Guyer, and Y. H. Sohn, J. Appl. Phys. **106**, 034912 (2009).
[22] M. W. Muller and R. S. Indeck, J. Appl. Phys. **75**, 2289 (1994).
[23] M. S. Leu, C. S. Tsai, C. S. Lin, and S. T. Lin, IEEE Trans. Magn. **27**, 5414 (1991).